



This is a repository copy of *Minimising microbubble size through oscillation frequency control*.

White Rose Research Online URL for this paper:  
<http://eprints.whiterose.ac.uk/129001/>

Version: Published Version

---

**Article:**

Brittle, S., Desai, P. [orcid.org/0000-0001-5266-0359](http://orcid.org/0000-0001-5266-0359), Ng, W.C. et al. (4 more authors) (2015) Minimising microbubble size through oscillation frequency control. *Chemical Engineering Research and Design*, 104. pp. 357-366. ISSN 0263-8762

<https://doi.org/10.1016/j.cherd.2015.08.002>

---

**Reuse**

This article is distributed under the terms of the Creative Commons Attribution (CC BY) licence. This licence allows you to distribute, remix, tweak, and build upon the work, even commercially, as long as you credit the authors for the original work. More information and the full terms of the licence here:  
<https://creativecommons.org/licenses/>

**Takedown**

If you consider content in White Rose Research Online to be in breach of UK law, please notify us by emailing [eprints@whiterose.ac.uk](mailto:eprints@whiterose.ac.uk) including the URL of the record and the reason for the withdrawal request.



[eprints@whiterose.ac.uk](mailto:eprints@whiterose.ac.uk)  
<https://eprints.whiterose.ac.uk/>

Contents lists available at [ScienceDirect](http://www.sciencedirect.com)

Chemical Engineering Research and Design

journal homepage: [www.elsevier.com/locate/cherd](http://www.elsevier.com/locate/cherd)


# Minimising microbubble size through oscillation frequency control

Stuart Brittle<sup>a,\*</sup>, Pratik Desai<sup>a</sup>, Woon Choon Ng<sup>b</sup>, Alan Dunbar<sup>a</sup>,  
Robert Howell<sup>b</sup>, Vaclav Tesař<sup>c</sup>, William B. Zimmerman<sup>a</sup>

<sup>a</sup> Department of Chemical & Biological Engineering, University of Sheffield, Sheffield, United Kingdom

<sup>b</sup> Department of Mechanical Engineering, University of Sheffield, Sheffield, United Kingdom

<sup>c</sup> Institute of Thermomechanics AS CR, v.v.i., Czech Academy of Sciences, Prague, Prague, Czech Republic

## ARTICLE INFO

### Article history:

Received 15 April 2015

Received in revised form 10 July 2015

Accepted 2 August 2015

Available online 8 August 2015

### Keywords:

Microbubbles

Process intensification

Transport phenomena

System design

Fluidic oscillator

Process optimisation

## ABSTRACT

Microbubbles are bubbles below 1 mm in size and have been extensively deployed in industrial settings to improve gaseous exchange between gas and liquid phases. The high surface to volume ratio offered by microbubbles enables them to enhance transport phenomena and therefore can be used to reduce energy demands in many applications including, waste water aeration, froth flotation, oil emulsion separations and evaporation dynamics. Microbubbles can be produced by passing a gas stream through a micro-porous diffuser placed at the gas–liquid interface. Previous work has shown that oscillating this gas stream can reduce the bubble size and therefore increase energy savings. In this work we show that it is possible to further reduce microbubble size (and consequently maximise the number of bubbles) by varying the frequency of the oscillating gas supply. Three different microbubble generation systems have been investigated; an acoustic oscillation system and a mesh membrane, a fluidic oscillator coupled to a single orifice membrane and a fluidic oscillator coupled to a commercially available ceramic diffuser. In all three bubble generation methods there is an optimum oscillation frequency at which the bubble size is minimised and the number of microbubbles maximised. In some cases a reduction in bubble size of up to 73% was achieved compared with non-optimal operating frequencies. The frequency at which this optimum occurs is dependent on the bubble generation system; more specifically the geometry of the system, the type micro-porous diffuser and the gas flow rate. This work proves that by tuning industrial microbubble generators to their optimal oscillation frequency will result in a reduction of microbubble size and increase their number density. This will further improve gaseous exchange rates and therefore improve the efficiency of the industrial processes where they are being employed to produce bubbles, leading to a reduction in associated energy costs and an increase in the overall economic and energetic feasibility of these processes.

© 2015 The Authors. Published by Elsevier B.V. This is an open access article under the CC BY license (<http://creativecommons.org/licenses/by/4.0/>).

## 1. Introduction

Bubbling systems have regularly been employed in industrial processes in order to achieve gaseous exchange of both mass and heat from gaseous phases to the liquid phase and

vice versa. More recently microbubbles have been shown to improve the efficiency of these gaseous exchange processes due to their higher surface area to volume ratio (Zimmerman et al., 2011a,b). Microbubbles can be generated by passing gas through a microporous diffuser at the gas–liquid interface or

\* Corresponding author. Tel.: +44 7888705187.

E-mail address: [s.brittle@sheffield.ac.uk](mailto:s.brittle@sheffield.ac.uk) (S. Brittle).

<http://dx.doi.org/10.1016/j.cherd.2015.08.002>

0263-8762/© 2015 The Authors. Published by Elsevier B.V. This is an open access article under the CC BY license (<http://creativecommons.org/licenses/by/4.0/>).

through other methods discussed in Zimmerman et al. (2011a). It has been shown that the gas pressure (and therefore energy input) required to do this can be significantly reduced if an oscillation is applied to the flowing gas stream prior to passing through the diffuser. Previous studies using oscillatory flow have shown improvement in topics such as microflotation (Hanotu et al., 2012), algal growth (Ying et al., 2013), wastewater aeration and treatment (Rehman et al., 2015) and oil-emulsion separations (Hanotu et al., 2013). Hanotu et al., used oscillated and non-oscillated air which showed a significant size reduction using oscillated air. This study reported reduction in bubble size from 1059  $\mu\text{m}$ , using a steady air flow system, to 84  $\mu\text{m}$ , with an oscillated air mechanism, using a diffuser with an average pore size of 38  $\mu\text{m}$  (Hanotu et al., 2012).

Surface area to volume ratio has been long understood to be extremely relevant in processes involving heat and mass transfer (Bird et al., 2007). The higher the ratio, the better the performance of the system. If the radius of a bubble is halved bubble volume will be reduced to 1/8 its original value and the surface area reduced to 1/4 its original value. Therefore the transfer coefficients which are proportional to the surface area to volume ratio will be increased by a factor of 2. Therefore if bubble sizes are reduced, in turn the process efficiency is improved due to better heat or mass transfer (Zimmerman et al., 2008).

Microbubbles provide unique opportunities due to their ability to be manipulated photo-acoustically therefore providing manoeuvrability (Ashkin, 1997; Lauterborn and Kurz, 2010), lower rise velocity meaning greater residence time (Zimmerman et al., 2013) and have their ability to be used as sensors (Darveau, 2011). Small (<8  $\mu\text{m}$ ) microbubbles have other potential applications in medicine such as theranostics (Liu et al., 2006). The reduced buoyancy and size of microbubbles <8  $\mu\text{m}$  means that they will not cause blockages in capillaries associated with larger bubbles. For most of these applications it is desirable to have a narrow size distribution. For example when applying photo-acoustic tweezing the microbubble manoeuvrability is size dependent, so having a narrow size distribution is hugely beneficial. For medical applications if a wider size distribution is generated the bubbles must be differentially centrifuged to select the desired size. This adds an additional process thereby increasing costs (Brodkey, 2004; Feshitan et al., 2009). Therefore there is considerable interest in being able to control and therefore reduce the size of microbubbles. In general being able to provide a narrow distribution of very small bubbles will result in increased efficiency and economics of the various processes that use microbubbles.

The first of the microbubble generating methods investigated here uses an acoustic speaker to oscillate the airstream before it flows through the diffuser. With this system it is very easy to explore a wide range of oscillation frequencies as the frequency is defined by the waveform played through the speaker. The two other microbubble generation systems use microfluidic devices known as a Tesar–Zimmerman fluidic oscillator (Jilek, 2013; Tesař, 2012; Tesař and Bandalusena, 2011; Zimmerman et al., 2011a,b, 2010) to generate the oscillation before the gas stream passes through two different diffusers, one with a single orifice and another with multiple orifices (mesoporous diffusers). The latter is most typical of the large scale microbubble generators being used in industry.

The Tesar–Zimmerman fluidic oscillator is a microfluidic device with no moving parts that creates a dynamic jet which alternates between two exit ports at a frequency determined by the feedback characteristics of the oscillator. This oscillatory flow is generated due to the adherence of the jet to one wall, caused by the Coanda effect, and its subsequent detachment and adherence to the opposite wall due to a switchover caused by pressure changes in the feedback loop. The gas stream from either or both of the exits can be passed through porous diffusers in order to engender microbubbles in an economical fashion. In this work a control loop has been used so that the operating frequency of the fluidic oscillator can be altered using this technique, which has been adequately described in Tesař and Bandalusena (2011). Clearly the orifice size in the microporous diffuser will play a significant role in determining the size of the bubbles produced (Clift et al., 1978). However, reducing the orifice size increases the pressure required to push the gas through the diffuser and therefore increases the energy requirements of the system. This shows that minimising the bubble size for a fixed diffuser geometry is of industrial relevance and highly beneficial if this results at no additional expenditure in energetics.

The motivation of this work was to investigate how bubble size varies as a function of oscillation frequency. From previous work (Zimmerman et al., 2011a,b, 2010, 2008) it is clear that applying an oscillation to the gas stream can help reduce bubble size and this was attributed to an increased rate of bubble ‘pinch off’ due to the oscillation. Three different microbubble generators are studied, exploring the size of the microbubbles generated as a function of the oscillation frequency when producing air bubbles in water. Exploring this relationship deepens the understanding of how to control microbubble production and therefore enables the required bubble sizes for their various industrial applications to be easily targeted economically. This work investigates if improvement is possible using three bubble generation systems all utilising oscillated gas flow streams. It is important to know how the frequency of the oscillating gas stream affects the size of the bubbles produced in order to further increase the impact of the oscillator on energy cost. This work investigates how frequency control affects microbubble generation using three different bubble generation systems.

## 2. Experimental methods

Three techniques to create bubbles using an oscillating air-flow are used in this study. The oscillation mechanism and the diffuser type i.e. mesh, single orifice membrane or multi-orifice diffuser (at the air water interface) are varied in these 3 methods.

- I. An acoustic oscillation system and a metal mesh membrane.
- II. The fluidic oscillator coupled to a single orifice membrane via a bespoke visualisation rig.
- III. The fluidic oscillator and a commercially available diffuser with an average pore size of 20  $\mu\text{m}$ .

For each of these techniques the oscillation frequency is controlled and the effect on the bubble size is observed.

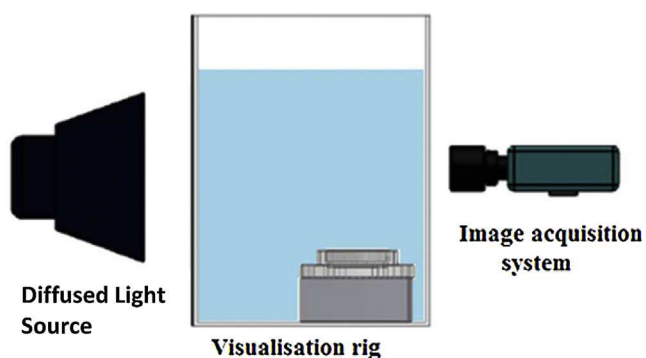


Fig. 1 – Image acquisition set up.

### 2.1. Imaging apparatus

The imaging techniques used in each of the three setups is the same. The camera, object and light source are placed in an orientation similar to that depicted in Fig. 1.

The light is generated by a ThorLabs White LED Array light source (LIU004) with an intensity of  $1700 \mu\text{W}/\text{cm}^2$  and emitted at a peak of 450 nm. The bright LED light source is diffused into a more uniform light using a white plastic translucent optical diffuser layer, before entering the bubble visualisation tank where the bubbles are produced and imaged. The tank was specifically designed for use with the high-speed camera, using a transparent quartz glass. The bubbles are imaged using a Pixelink PL742 camera in setup I with an adjustable magnification lens. In setups II & III a Photron FastCam SA3 was used with a Nikon AF Nikkor (24–85 mm 1:2.8–4D) lens.

The bubbles were imaged and sized for each of the three methods at various oscillation frequencies. The bubbles imaged for each of the three methods (I–III) vary both in the number of bubbles produced and the size and shape due to the nature of the mesh, membrane or diffuser and the extent

of magnification. Examples of the images produced using the three methods are given in Fig. 2.

### 2.2. Image analysis

The images of the illuminated bubbles were captured and these images analysed using bespoke image analysis software, in order to determine the mean average bubble size using the equation shown:

$$D[1, 0] = \frac{\sum_1^n D}{n}$$

where  $D$  is the diameter of an individual bubble and  $n$  is the total number of bubbles. The pixel size for each experimental setup was calibrated by imaging an object of known size. The  $D[1, 0]$  method of calculating average bubble diameter is chosen for simplicity, and to quickly represent any changes in bubble diameter that may occur as a result of system parameter alterations.

The bubble density in a liquid is an important parameter because various applications require different bubble sizes. For example biomedical imaging applications will require a different bubble size to that of microflotation. This paper addresses a general optimisation for bubble generation under oscillatory flow. Comparisons to bubble size with and without oscillated flow have been demonstrated previously (Hanotu et al., 2012; Zimmerman et al., 2011a,b), along with associated bubble density and size distribution. It is also important to note that no surfactant was used in this study as only generated bubbles are of interest, not those retained.

The ceramic diffuser used in setup III has a porous structure at which bubbles are created and requires a relatively large air pressure. The result is that the diffuser forms large clouds of bubbles, similar to those reported by Hanotu et al. (2012). The fluidic oscillator—single orifice system requires a lower air flow rate and produces fewer bubbles, one at a time, through a single orifice and consequently this method produces a much

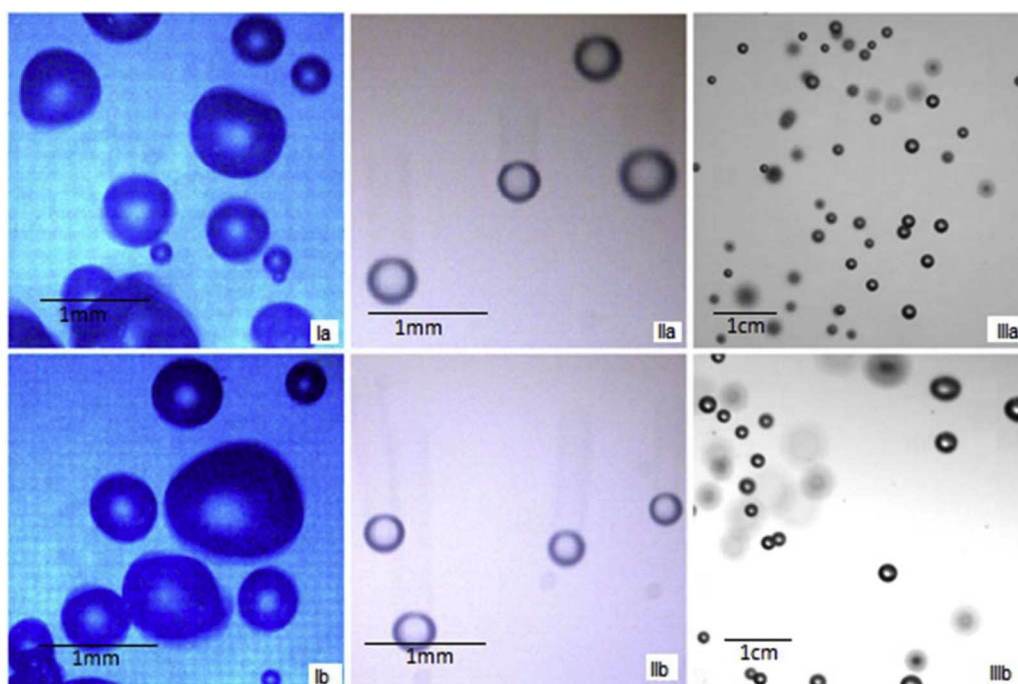


Fig. 2 – Two bubble images for each of the three methods are provided. Left: images from the acoustic oscillation mesh method (I). Middle: bubble images from the fluidic oscillator single orifice method (II). Right: bubble images from the fluidic oscillator diffuser method (III).



**Fig. 3 – The three porous media used in this study. Left, the nickel mesh. Centre, the single orifice. Right, the porous ceramic diffuser imaged using SEM.**

lower number density of bubbles. The acoustic oscillation with mesh system is also a relatively low airflow rate system compared with that of the ceramic diffuser system due to the reduced number of pores and produces considerably fewer bubbles as a result. However, the mesh is able to produce more than one bubble at a time, due to the numerous paths for air to flow through its grating and therefore produces an intermediate number density of bubbles compared to the other two setups. Images, acquired through differing techniques, of these porous media can be seen in Fig. 3.

Since the bubble density varies between the three methods it is also necessary to take different numbers of images to gain an appropriately similar number of bubbles to analyse for the mean bubble diameter calculation. The degree of magnification varies from one set-up to the next and therefore reference images have been used to correctly size bubbles from these images.

### 2.3. Bubble generation techniques

#### 2.3.1. An acoustic oscillation system and mesh

The acoustic oscillation system is a bespoke device made to extensively study a wide range of oscillation frequencies. The air oscillation is produced using an acoustic speaker and therefore the frequency of output is easily controlled. A large range of frequencies with small interval step sizes can be studied easily compared to the intervals available when using the inherently mechanical fluidic oscillator systems described below. A virtual signal generator was used to produce waveforms using bespoke software developed in Lab-View. The waveforms were used to drive the acoustic speaker using a standard amplifier controlled by the computer's soundcard. Variation in the frequency and waveform shape could therefore be easily controlled within the software. The saw-tooth wave was observed to aid the bubble pinch off best,

as compared to sinusoidal, square and triangular waveforms. The system set up is shown in Fig. 4.

The compressed air supply passes through a control valve followed by a pressure regulator to ensure a constant pressure. The flow controller (Bronkhurst, EL-FLOW), positioned before the acoustic bubble generator (ABG), maintains a steady influx of air into the ABG. The flow rate is kept constant during frequency sweeps of the ABG in order to isolate effects relating to frequency on the bubble size. Further frequency sweeps are performed when the flow rate is changed. The ABG superimposes an oscillation onto the flowing airstream via a signal generator and then funnels the pulsed air towards the mesh membrane at the air/water interface. The mesh used in this experiment is nickel with a 200 grating, giving spacing of approximately  $130\ \mu\text{m}$ . The depth of the water column above the mesh at the mesh/air/water intersection, is kept sufficiently low such that the water pressure does not overcome the surface tension inside the porous mesh and therefore inhibits the backflow of water into the ABG, even without any air flow.

The mean bubble size is plotted against the frequency of the oscillation (pulsed air), in Fig. 5 for the Acoustic Oscillation and Mesh system, in Fig. 7 for the fluidic oscillator—single orifice method and in Fig. 9 for the fluidic oscillator—diffuser method. The bubbles sizes have been normalised, with respect to the largest bubbles in a data set, simply to allow for easier comparison between results. The normalisation factors are given in the figure captions.

The results for the acoustic oscillation and mesh system are shown in Fig. 5. Each graph in Fig. 5 represents a different type of mesh at the air/water interface of the system or flow rate. All the plots illustrate that there is a distinctive minimum in each of the data sets, representing a 'sweet spot' of speaker oscillation that creates the smallest average diameter bubbles ( $D[1,0]$ ). The difference between Mesh 1 and

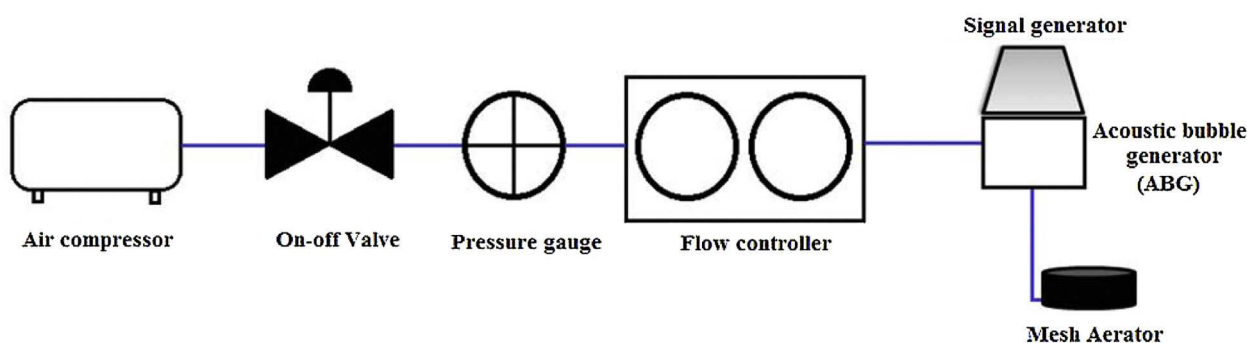


**Fig. 4 – Set up of the acoustic oscillation system and mesh.**

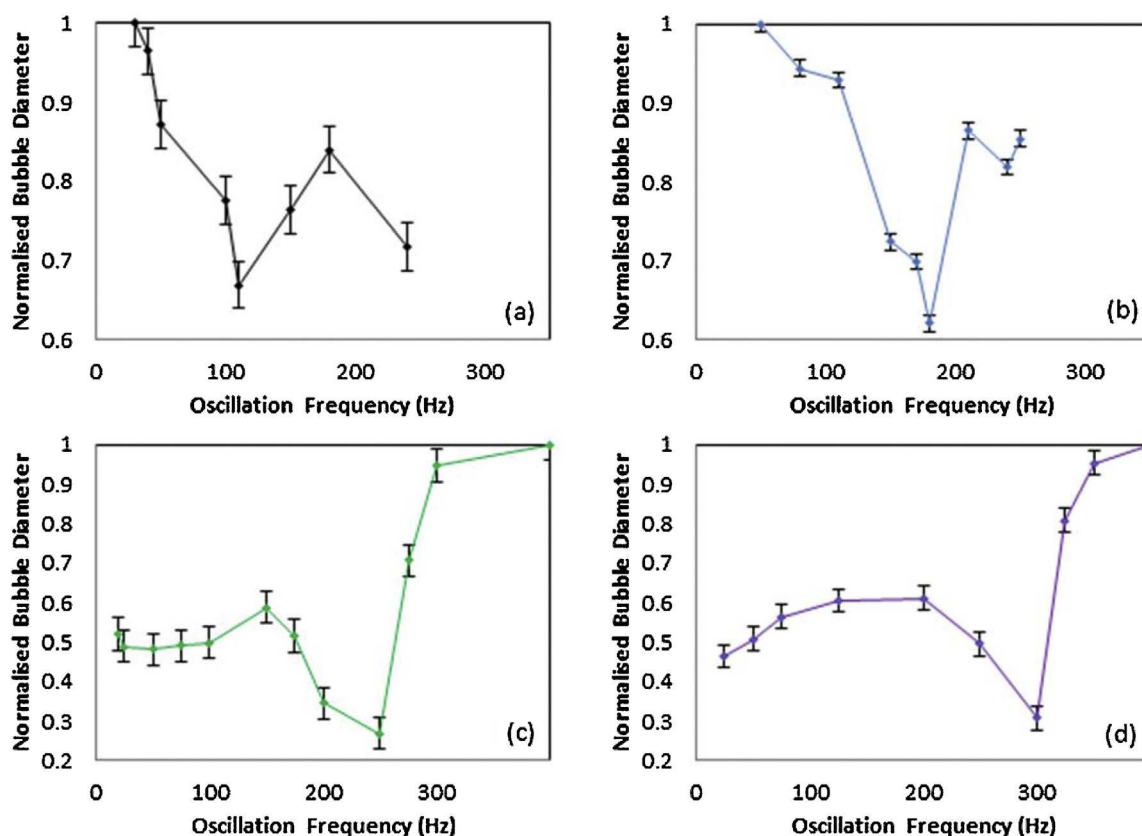


**Fig. 5** – Data taken using the acoustic oscillation–mesh technique. Mesh 1 with a flow rate of 5 ml/min (a), mesh 1 with a flow rate of 25 ml/min (b), mesh 2 with a flow rate of 5 ml/min (c), and mesh 2 with a flow rate of 10 ml/min (d). 861  $\mu\text{m}$  (a), 3190  $\mu\text{m}$  (b), 1141  $\mu\text{m}$  (c) and 2104  $\mu\text{m}$  (d) are the normalising factors.

Mesh 2 is the grating size. Mesh 1 has a 200 grating whereas Mesh 2 is 250, thus slightly reducing the pore size in Mesh 2 but increasing the number density of pores.

It is observed that as flow rate increases in this system, the frequency that results in the minimum bubble diameter, also increases. This is deduced by comparing Fig. 5(a) with Fig. 5(b), where an increase in flow rate from 5 ml/min to 25 ml/min increases the optimum frequency from 110 Hz to 180 Hz. And also by comparing Fig. 5(c) with Fig. 5(d), where an increase in flow rate from 5 ml/min to 10 ml/min increases the optimum frequency from 250 Hz to 300 Hz. The maximum reduction in average bubble diameter using this experimental method is  $\sim 73\%$ .

### 2.3.2. Fluidic oscillator—Single orifice method

The setup for the fluidic oscillator—single orifice method is shown in Fig. 6. The inlet air flow enters the system through a shut off valve. The pressure and global flow rate are controlled by a pressure regulator and rotameter respectively (Norgren, Omega Instruments). The rotameter modulates inlet flow rate, preparing the airflow prior to entering the fluidic oscillator. The fluidic oscillator creates pulsed airflow at both the outlets (Tesař, 2007). One outlet is connected through a single orifice membrane at the base of the bubble visualisation tank and the other is vented to atmosphere through a bleed valve (in an industrial setting, the second outlet would feed a second bubble generating diffuser or an array of diffusers). This will work as long as both of them are ‘balanced’ together. It is imperative that both outlets are suitably balanced to maintain the oscillation for this no-moving part fluidic switching device since it is a bistable valve and therefore bistability needs to be maintained. There is a second bleed valve on a branch of the outlet

being fed to the single orifice membrane which is used to control the total amount of gas being fed to the membrane. This is necessary to allow appropriate flow into the bubble visualisation tank whilst simultaneously allowing the fluidic oscillator to oscillate at the required frequencies. A pressure transducer Impress G1000 (Range 0–1 bar (g)) is fitted in the supply line to the diffuser in order to accurately measure the frequency of air of the system. The input flow rate used as standard through the fluidic oscillator is 65 l/min with over 99.9% being vented in order to be used with the single orifice membrane and the inlet pressure is maintained at 0.5 bar (g). The actual flow rate entering bubble visualisation tank varies slightly depending on the fluidic oscillator frequency due to changes in the feedback loop and ranges between 0.2 ml/m and 0.5 ml/m. The frequency of the fluidic oscillator depends upon the input flow rate and the length of the feedback loop. Since the input flow rate and the system is kept constant, the feedback loop length is used as the parameter determining the frequency of the oscillator. The membrane used in this study is a single 30  $\mu\text{m}$  orifice membrane procured from Potomac Photonics Inc.

Fig. 7 shows the mean bubble diameter as a function of oscillation frequency for setup II the fluidic oscillator—single orifice method, performed at the two different flow rates, 2.8 ml/min and 2.3 ml/min. Both flow rates demonstrate a distinctive minimum average bubble diameter. These minima occur at different frequencies (147 Hz for the 2.8 ml/min data and 237 Hz for the 2.3 ml/min data) which is attributed to the different flow rates. The change in flow rates results in a change in the dynamics of the system. A maximum of  $\sim 15\%$  reduction of average bubble diameter is observed using this fluidic oscillator—single orifice experimental system. Single orifices are a useful way of studying the phenomena

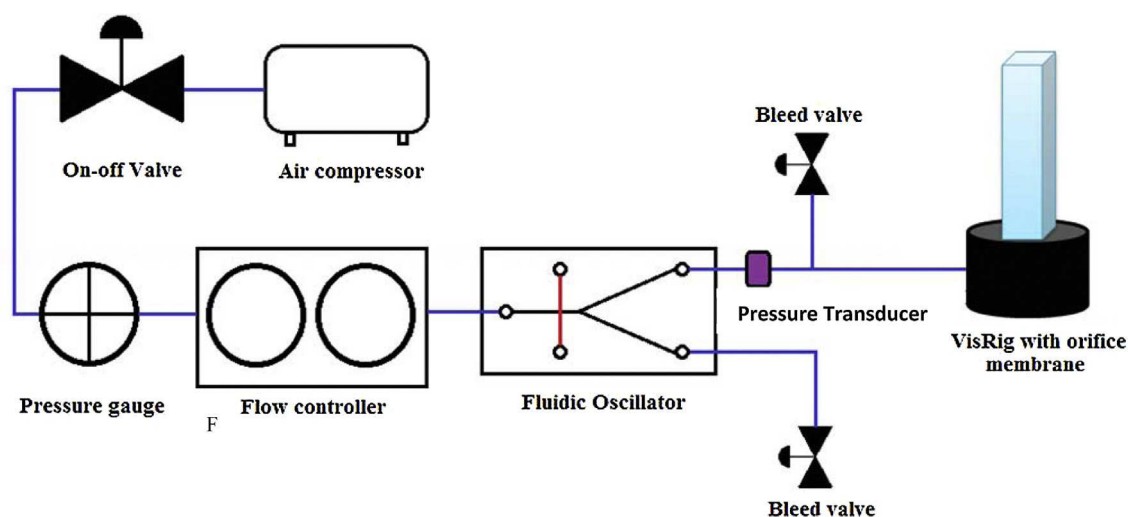


Fig. 6 – Set up for the fluidic oscillator—single orifice method.

associated with bubble formation and dynamics using a reduced bubble sample density compared to cloud bubble generation associated with other techniques, yet still allowing the validity of the hypothesis to be explored. In this case finding the dependency of bubble size on oscillation frequency ought to be easily measurable using this technique. The lower bubble density also simplifies the automated image analysis greatly since few bubbles overlap, images are clearer as the intended focal plane is more predictable and there are fewer bubble–bubble interactions.

### 2.3.3. Fluidic oscillator—Application of the fluidic oscillator on a mesoporous diffuser

The methodology for creating pulsed air in this setup is identical to that described in Part II fluidic oscillator—single orifice method above. However, different setup parameters are needed and different frequencies are generated because a ceramic diffuser is used at the air water interface (rather than the single orifice membrane) and therefore the system dynamics have changed.

The air takes the same route to the fluidic oscillator, as that described above but upon exiting the oscillator both outlets are fed to separate diffusers. Due to the nature of the porous diffuser material the pressure required to push air through its pores is higher (approximately 1 bar (g)). A larger number of bubbles are formed due to the scaled up process—(when compared to a single orifice). This provides a larger sample size for experimental significance.

The bleed valves perform the same function as for the fluidic oscillator—single orifice method which is to balance the outlet legs of the oscillator (it needs to perform bi-stably) whilst feeding an appropriate amount of flow into the diffuser. The diffusers are placed directly in a bubble visualisation tank and therefore it is necessary to measure the frequency at one of the oscillator outlets using an accelerometer (ADXL345) and calibrated using an Impress G1000 Pressure Transducer. Four flow rates (0.1l/min, 0.15l/min, 0.2l/min & 0.35l/min) were used with frequency sweeps. Both the diffusers were kept under similar conditions and were matched for performance and found to be equi-responsive with less than 5% variation in performance (Fig. 8).

Fig. 9 shows the graphs of the data taken using the fluidic oscillator applied on a mesoporous diffuser at various inlet flow rates. Again each of the graphs show a distinctive minimum average bubble size throughout the frequency sweep. The mean bubble size minimum for this system appears at much lower oscillation frequencies, compared to those taken with the fluidic oscillator—single orifice method. This effect is due to the difference in the set up of the system, such as the Chambre volume as well as the change in dynamics i.e. single bubble generation and bubble cloud formation. The ceramic diffusers used herein present a different scenario to the bubbles formed through the single orifice. The pressure of the system is higher, the volume of the diffuser is larger and these factors affect bubble formation. From the data shown in Fig. 9 we can observe that an increasing inlet flow rate also

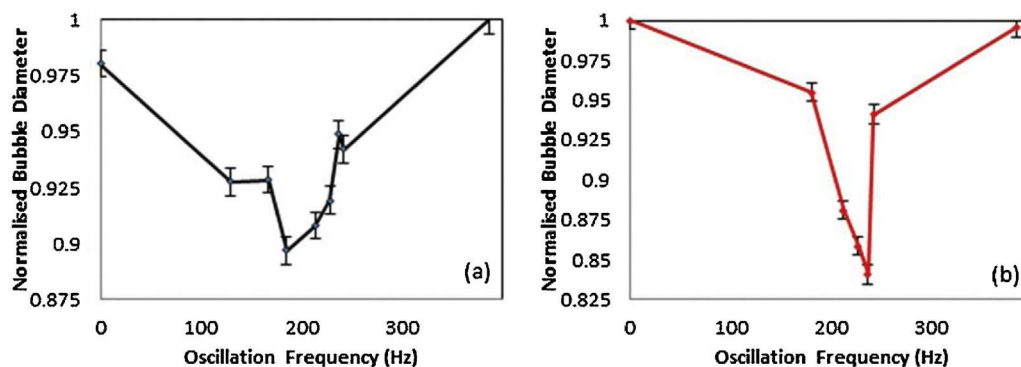


Fig. 7 – Data taken using the fluidic oscillator—single orifice method. With actual flow rates of 2.8 ml/min (a) and 2.3 ml/min (b). 649  $\mu\text{m}$  (a) and 755  $\mu\text{m}$  (b) are the normalising factors.

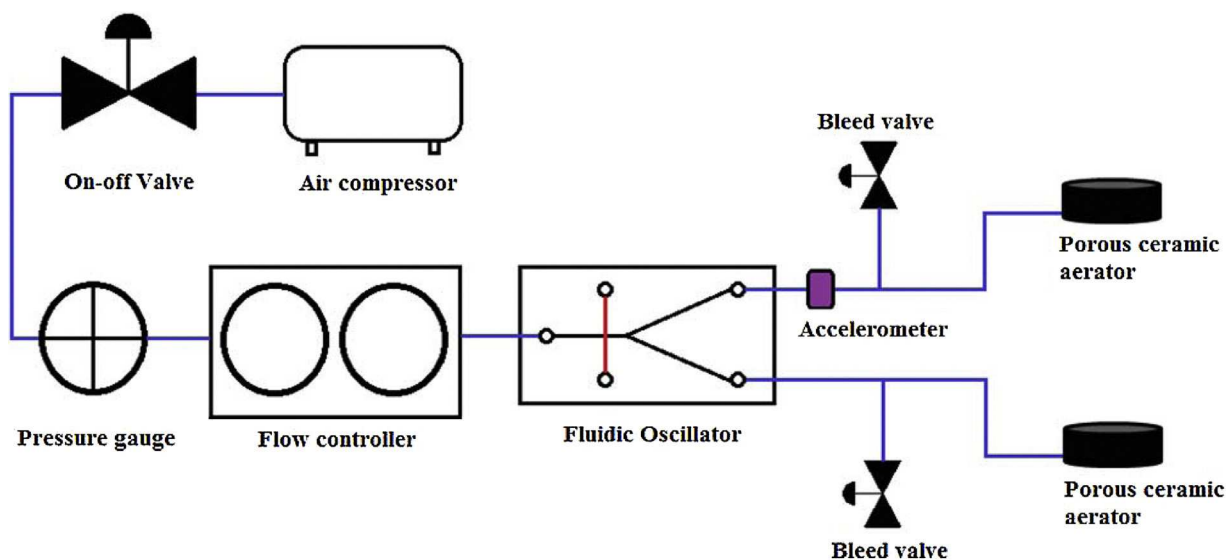


Fig. 8 – Set up for the fluidic oscillator—diffuser method.

increases the average bubble diameter. Occurring at 122 Hz, 124 Hz, 124 Hz and 125 Hz, for flow rates 0.1 l/min, 0.15 l/min, 0.2 l/min and 0.35 l/min, respectively. The minimum average bubble diameter ( $D[1,0]$ ) has been shown to reduce by up to ~47% for this particular experimental method. All of the data plotted in Fig. 9 illustrate a high dependency of average bubble size on oscillation frequency and therefore the importance of knowing the where this optimum frequency for minimising bubble size is highlighted.

We have been able to show that for each of the three bubble systems there is an optimum frequency at which the mean bubble size is minimised. This is significant because current

practice when employing microbubbles to improve the efficiency of gaseous exchange in industrial processes is simply to use a non-optimised fluidic oscillator operating at a default frequency. All systems have used various flow rate settings. The use of these specific flow rates is dependent on the orifice area or throughput of the bubble generators. This study shows that these type of system have the ability to be tuned in order to reduce the mean microbubble size, by up to ~73%. The reduction in bubble size upon optimising the frequency was most pronounced for the acoustic system relative to the bubble size formed i.e. percentage reduction. This is attributed to the much finer control of speaker frequency that is possible

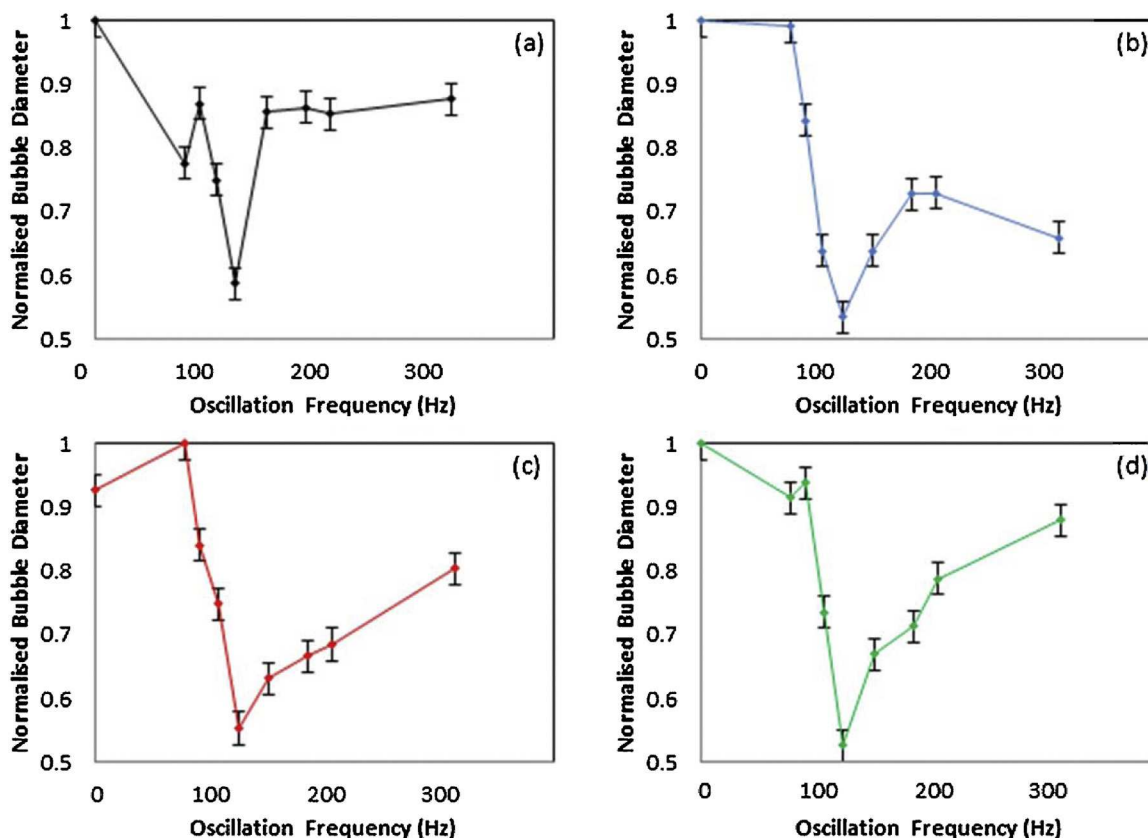
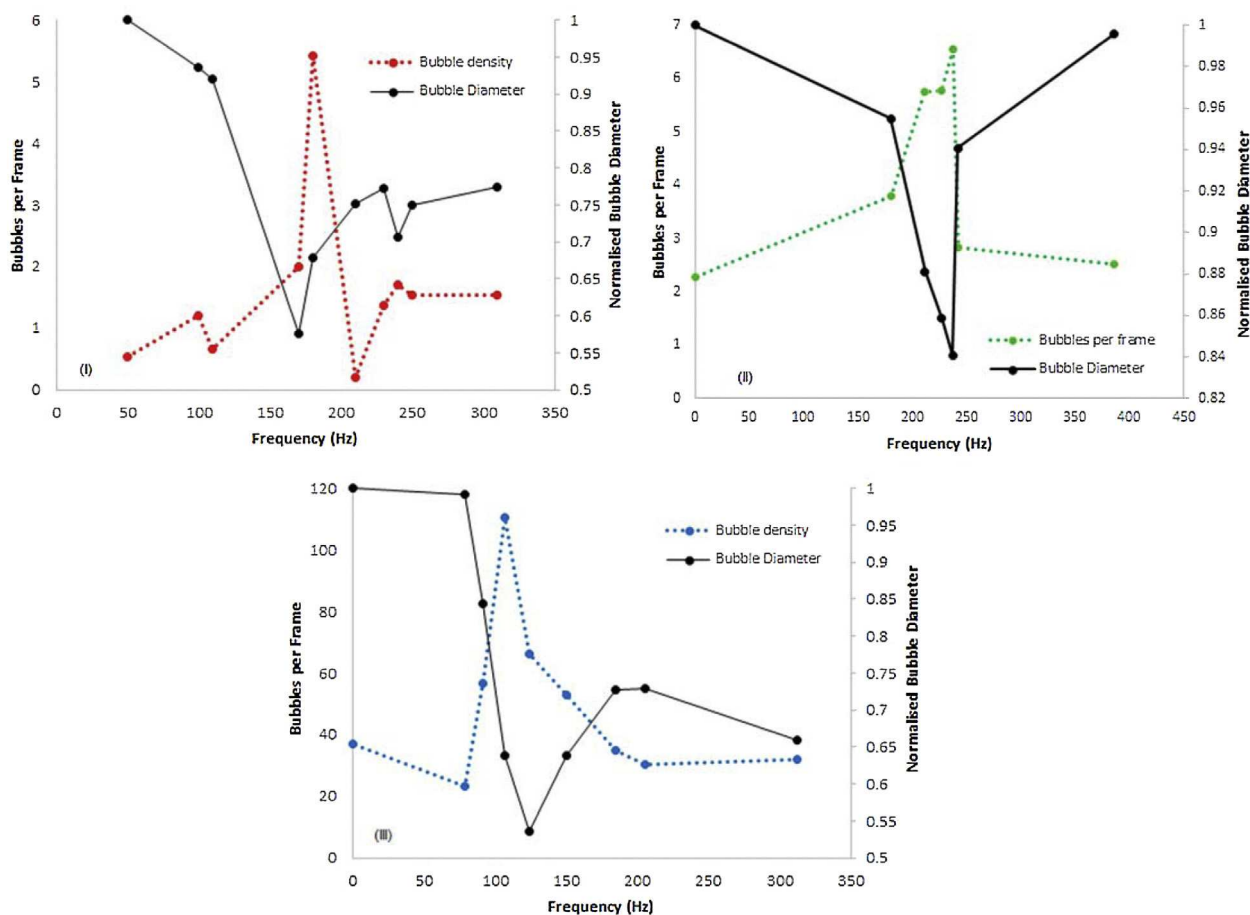


Fig. 9 – Data taken using the fluidic oscillator—diffuser method. 0.1 l/min (a), 0.15 l/min (b), 0.2 l/min (c) and 0.35 l/min (d). 580  $\mu\text{m}$  (a), 686  $\mu\text{m}$  (b), 682  $\mu\text{m}$  (c) and 776  $\mu\text{m}$  (d) are the normalising factors.





**Fig. 10** – The bubble number density is displayed alongside the bubble diameter as a function of frequency. The acoustic oscillation–mesh membrane technique (I) using mesh 2 and a flow rate of 25 ml/min, the fluidic oscillator–single orifice method (II) using 2.3 ml/min flow rate, and the fluidic oscillator–ceramic diffuser method (III) at 0.15 ml/min.

in this setup. It implies that by further optimising the length of the feedback loops used, in the other two fluidic oscillator setups, greater reductions in bubble size could be realised there too.

Fig. 10 is used as an example of bubble number density figures. It shows an example for each method and plots both bubble size and densities with respect to frequency. Fig. 10 clearly shows that the optimum frequency for producing smaller bubbles also correlates to an increase in number of bubbles. This is expected because the flow rate, or total gas throughput, remains constant yet the average bubble size decreases and larger numbers of bubbles are produced.

### 3. Discussion

Bubbles are formed by passing gas through a small orifice into a liquid, when sufficient gas has entered the bubble to force it to pinch off from the orifice. Bubble pinch off and bubble generation under oscillatory flow has been elucidated well in publications by Tesař (2014,2013b,2013c) and Zimmerman et al. (2011a,b). This is different from the bubble generation via third harmonic excitation explained by Tesař (2013a) but the general reasoning remains the same. In order to produce very small bubbles it is beneficial to force bubble ‘pinch off’ to occur as frequently as possible. Whether or not bubble ‘pinch off’ occurs is determined by several competing factors. The buoyancy of the bubble and the momentum of the gas filling the bubble will encourage it to pinch off whilst the surface tension of the air–water interface will hinder pinch off, instead

promoting the bubble to grow larger minimising the surface curvature. Eventually as the bubble size increases the curvature of the interface will change from a dome shape to a more spherical shape. The sphere will continue to grow becoming larger than the orifice at which point the curvature near the orifice will begin bending outwards and eventually will become so extreme pinch off occurs. Clearly the flow rate of gas passing through the orifice will determine the amount of gas entering the forming bubble and its velocity. Pinch off will occur when the buoyancy forces can overcome the surface wetting force, which acts to hold back the flow of gas. The wetting characteristics determined by the hydrophobicity of the orifice material will determine whether or not the surface wetting force is minimised by lateral spreading of the forming bubble. Hydrophilic surfaces will result in smaller bubbles being produced because the water will preferentially sit next to the orifice material forcing the bubble to adopt a smaller radius of curvature therefore encouraging early pinch off (Kukizaki and Wada, 2008).

The effect of frequency on bubble size observed in this paper and the distinct sweet spot in frequency can be explained in terms of small air pulses entering the forming bubble. If the frequency is low the pulse will be longer and therefore contain more gas. This will mean that sufficient gas to force pinch off will be delivered in a single pulse. If on the other hand the frequency is high insufficient gas is delivered per pulse and it may take two or more pulses before pinch off can occur. If however the frequency is at the optimum where the amount of gas entering the bubble per pulse is

sufficient to create a bubble then pinch off may occur during every pulse. The lifting force associated with the momentum of the gas delivered during such a pulse will add to the buoyancy force and therefore permit smaller bubbles than would otherwise be permitted to be formed. The combination of the bubble buoyancy and gas momentum can overcome the surface tension effects. Frequencies just above the optimum will deliver smaller momentum contributions per pulse and therefore results in increasing bubble sizes above the optimum frequency. At even higher frequencies above the sweet spot the increased frequency means that each pulse contains lower amounts of air and less momentum is delivered to thrust the bubble away from the membrane and overcome the surface tension. Thus, the smaller bubble fails to detach and can only do so when further pulses of air enter the bubble, increasing the bubble volume and its buoyancy force before detaching. Frequencies just below the optimum will deliver more than enough gas per pulse for pinch off to occur and as a result the bubbles will grow throughout the pulse resulting in larger sized bubbles.

An alternative way to think of the oscillatory effect is in terms of pressure fluctuations. During the on pulse, air pressure is high and air will flow into the forming bubble pushing outwards against the surface tension. If this bubble grows sufficiently large to be close to pinch off the reduction in pressure during the off pulse will cause a perturbation of the bubble size which may induce premature pinch off (compared to continuous flow conditions) resulting in smaller bubbles.

This work has shown that it is necessary to tailor the oscillation frequency to the type of microbubble generation system being used in order to minimise the bubble size generated. Therefore fluidic oscillators for microbubble production should be built with a particular application in mind and engineered and designed to create a frequency optimised for that system.

This paper has explored three different oscillatory systems and we have demonstrated that all these systems have a frequency sweet spot. Wastewater aeration and microflotation systems have previously benefitted by oscillatory flow demonstrated by [Rehman et al. \(2015\)](#) and [Hanotu et al. \(2012\)](#). Our reported oscillation tuning can further improve the performance of these systems.

#### 4. Conclusion

This work has proved the existence of a frequency optimum for microbubble generation using oscillatory air flow through a diffuser where the bubbles produced are significantly smaller in size and correspondingly greater in number than elsewhere in the frequency range. Application of the optimum frequency can reduce bubble sizes by up to ~73%. The occurrence of an optimum frequency to minimise bubble size is observed in all of the systems studied. It is predicted that the same should apply for any bubble generation system undergoing oscillatory airflow.

This discovery of bubble size reduction at the optimal oscillation frequency is important because it has the potential to improve process efficiencies, involving the use of microbubbles as heat and or mass transfer vehicles, simply by altering the oscillation frequency, thus requiring no further power input or system modifications, only to tune those oscillators already in place.

#### Acknowledgements

This work was carried out as part of the “4CU” programme grant, aimed at sustainable conversion of carbon dioxide into fuels, led by The University of Sheffield and carried out in collaboration with The University of Manchester, Queens University Belfast and University College London. The authors acknowledge gratefully the Engineering and Physical Sciences Research Council (EPSRC) for supporting this work financially (Grant no. EP/K001329/1). The authors would also like to acknowledge the support provided by Elliot Gunnard and Andrew “Andy” Patrick from the technical workshop at the Department of Chemical & Biological Engineering, University of Sheffield.

#### References

- Ashkin, A., 1997. [Optical trapping and manipulation of neutral particles using lasers](#). *Proc. Natl. Acad. Sci. U.S.A.* 94, 4853–4860.
- Bird, R.B., Stewart, W.E., Lightfoot, E.N., 2007. [Transport Phenomena](#). Wiley, Singapore.
- Brodkey, R., 2004. [The Phenomena of Fluid Motions](#). Brodkey Pub, Columbus, Ohio.
- Clift, R., Grace, J.R., Weber, M.E., 1978. [Bubbles, Drops, and Particles](#). Academic Press, Dover Publications, New York.
- Darveau, C.T., 2011. [Measuring Blood Pressure Using Microbubbles and Ultrasound](#). Master of Medical Biophysics, University of Toronto, Toronto.
- Feshitan, J.A., Chen, C.C., Kwan, J.J., Borden, M.A., 2009. [Microbubble size isolation by differential centrifugation](#). *J. Colloid Interface Sci.* 329, 316–324.
- Hanotu, J., Bandulasena, H.C., Zimmerman, W.B., 2012. [Microflotation performance for algal separation](#). *Biotechnol. Bioeng.* 109, 1663–1673.
- Hanotu, J., Hemaka Bandulasenab, H.C., Yen Chiuc, T., Zimmermana, W.B., 2013. [Oil emulsion separation with fluidic oscillator generated microbubbles](#). *Int. J. Multiphase Flow* 56, 119–125.
- Jilek, V.T.M., 2013. [Integral Fluidic Generator of Microbubbles](#). *Colloquium Fluid Dynamics 2013*. Institute of Thermomechanics AS CR, Prague.
- Kukizaki, M., Wada, T., 2008. [Effect of the membrane wettability on the size and size distribution of microbubbles formed from Shirasu-porous-glass \(SPG\) membranes](#). *Colloids Surf., A: Physicochem. Eng. Aspects* 317, 146–154.
- Lauterborn, W., Kurz, T., 2010. [Physics of bubble oscillations](#). *Rep. Prog. Phys.* 73, 106501.
- Liu, Y., Miyoshi, H., Nakamura, M., 2006. [Encapsulated ultrasound microbubbles: therapeutic application in drug/gene delivery](#). *J. Controlled Release* 114, 89–99.
- Rehman, F., Medley, G.J.D., Bandulasena, H., Zimmerman, W.B.J., 2015. [Fluidic oscillator-mediated microbubble generation to provide cost effective mass transfer and mixing efficiency to the wastewater treatment plants](#). *Environ. Res.* 137, 32–39.
- Tesař, V., 2007. [Pressure-Driven Microfluidics](#). Artech House, London.
- Tesař, V., 2012. [Microbubble generation by fluidics. Part I: Development of the oscillator](#). In: *Colloquium Fluid Dynamics 2012*, Prague, Czech Republic.
- Tesař, V., 2013a. [Microbubble generator, excited by fluidic oscillator's, third harmonic frequency](#). *Chem. Eng. Res. Des.* 92 (9), 1603–1615.
- Tesař, V., 2013b. [Microbubble smallness limited by conjunctions](#). *Chem. Eng. J.* 231, 526–536.
- Tesař, V., 2013c. [Shape oscillation of microbubbles](#). *Chem. Eng. J.* 235, 368–378.
- Tesař, V., 2014. [Mechanisms of fluidic microbubble generation. Part II: Suppressing the conjunctions](#). *Chem. Eng. Sci.* 116, 849–856.

- Tesař, V., Bandulasena, H., 2011. [Bistable diverter valve in microfluidics](#). *Exp. Fluids* 50, 1225–1233.
- Ying, K., Gilmour, D.J., Shi, Y., Zimmerman, W.B., 2013. [Growth enhancement of \*Dunaliella salina\* by microbubble induced airlift loop bioreactor \(ALB\)—the relation between mass transfer and growth rate](#). *J. Biomater. Nanobiotechnol.* 4, 1–9.
- Zimmerman, W.B., Al-Mashhadani, M.K.H., Bandulasena, H.C.H., 2013. [Evaporation dynamics of microbubbles](#). *Chem. Eng. Sci.* 101, 865–877.
- Zimmerman, W.B., Hewakandamby, B.N., Tesař, V., Bandulasena, H.C.H., Omotowa, O.A., 2010. [On the design and simulation of an airlift loop bioreactor with microbubble generation by fluidic oscillation](#). *Int. Sugar J.* 112, 90–103.
- Zimmerman, W.B., Tesař, V., Butler, S., Bandulasena, H.H., 2008. [Microbubble generation](#). *Recent Patents Eng.* 2, 1–8.
- Zimmerman, W.B., Tesař, V., Bandulasena, H.C.H., 2011a. [Towards energy efficient nanobubble generation with fluidic oscillation](#). *Curr. Opin. Colloid Interface Sci.* 16, 350–356.
- Zimmerman, W.B., Zandi, M., Bandulasena, H.H., Tesař, V., Gilmour, D.J., Ying, K., 2011b. [Design of an airlift loop bioreactor and pilot scales studies with fluidic oscillator induced microbubbles for growth of a microalgae \*Dunaliella salina\*](#). *Appl. Energy* 10 (8), 3357–3369.